PNAS

Supporting Information for
Polarizing agents beyond pentacene for efficient triplet dynamic nuclear polarization in glass matrices

Keita Sakamoto, Tomoyuki Hamachi , Katsuki Miyokawa, Kenichiro Tateishi, Tomohiro Uesaka, Yuki Kurashige, Nobuhiro Yanai

Yuki Kurashige, Nobuhiro Yanai
Email: kura@kuchem.kyoto-u.ac.jp , yanai@mail.cstm.kyushu-u.ac.jp

This PDF file includes:

Supporting Information Text

Materials and Methods

Materials

All reagents and solvents were used without further purification unless otherwise noted. 6,13-pentacenedione, benzothiophene, thiophene, benzofuran, butyllithium (2.6 mol/L hexane solution), *o*-terphenyl (OTP) and pentacene (purified by sublimation) were purchased from TCI. Dehydrated THF and sodium iodide were purchased from Wako. 6,13-diphenylpentacene and sodium hypophosphite hydrate were purchased from Sigma Aldrich. Acetic acid, $Sn_2Cl_2 \cdot 2H_2O$ was purchased from KISHIDA. OTP was purified by zone melting. 6,13-bis(benzo[b]thiophen-2-yl)pentacene (DBTP), 6,13-di(thiophen-2-yl)pentacene (DTP) and 6,13-di(benzofuran-2-yl)pentacene (DBFP) were synthesized according to the reported methods.[1] For the ESR and triplet-DNP samples, each polarizing agent was mixed with a matrix (*β*-estradiol, o-terphenyl). After grinding the mixture, resulting powder was inserted into an ampoule and sealed under degassed. The sealed ample was heated to 453 K for *β*-estradiol and 333 K for OTP. The resulting melt was rapidly cooled with liquid nitrogen. Obtained glassy solids were taken out from the ampoule and ground with a mortar.

General characterizations

^{1}H NMR (400 MHz) spectra were measured on a JEOL JNM-ECZ400 spectrometer. Elemental analysis was carried out by Yanaco CHN Corder MT-5 at the Elemental Analysis Center of Kyushu University. UV-vis absorption spectra were measured by JASCO V-670 and V-770 spectrophotometers. Solution samples were measured by the transmission method with a cell length of 1 cm, and solid samples were measured by the diffuse reflection method on a glass plate. Absolute fluorescence quantum yields were measured with an integrating sphere using HAMAMATSU C10027-01 multichannel analyzer. Time-resolved photoluminescence lifetime measurements were performed using a time-correlated single photon counting lifetime spectrometer (HAMAMATSU Quantaurus-Tau C11367-21, C11567-02, M12977-01). Zonemelt refining was performed using a MiniZone II Zone Refiner. Transient absorption measurements were conducted by using a UNISOKU TSP-2000.

Time-resolved ESR

Time-resolved ESR measurements were performed at room temperature on home-build system described in detail in our previous report.[2] Samples were photoexcited with a 527 nm pulsed laser (Tolar-527, Beamtech Optronics) in a dielectric resonator inside an electromagnet (MC160-60G-0.8T, Takano Original Magnet). Laser pulse width is about 200 ns. The repetition rate and laser power were set to 100 Hz and 0.3 W. ESR spectra of the photoexcited triplet were obtained from the sum of the signal intensities during the 5 μs after photoexcitation. The resonance frequency of the used cavity resonator was 9 GHz and the Q-value was about 2750. Microwaves of 1 mW were generated (SG24000H, DS Instruments), amplified by a power amplifier (ALN0905-12-3010, WENTEQ Microwave Corp) and converted to DC by a diode detector (DHM185AB, Herotek). ESR signals were amplified and noise was cut using two amplifiers (SA-230F5, NF ELECTRONIC INSTRUMENTS, 5305 differential amplifiers, NF ELECTRONIC INSTRUMENTS). ESR signals was detected by an oscilloscope (DSOX3024T, Keysight). ESR spectra were analyzed in MATLAB version R2019b (The Mathworks, Inc.).

Triplet-DNP experiment

Home-built triplet-DNP setup was described previously in detail,[2] which consists of an electromagnet (MC160-60G-0.8T, Takano Original Magnet), microwave resonator, coil for magnetic field sweep, and pulsed laser (Tolar-527, Beamtech Optronics). The sequence control and NMR signal detection were performed by OPENCORE NMR spectrometer.[3] The powder samples were inserted in glass capillaries (FPT-220, FUJISTON, diameter 2.2 mm, inner diameter 1.4 mm) and sealed under degassed.

The laser repetition frequency was set to 500 Hz, output power to 8.4 W, and pulse length to 200 ns. Continuous microwaves were generated by SG24000H (DS Instruments) and converted to

pulsed waves using a pin diode (S1517D, L3HARRIS). The pulse wave was amplified by a power amplifier (AMP4081P-CTL, EXODUS ADVANCED COMMUNICATIONS) and sent to the resonator via coaxial cable at a power of approximately 50 W. The magnetic field was swept by applying an amplified triangular wave to a copper wire installed in the resonator. The source triangular wave was generated from a function generator (WF1974, NF ELECTRONIC INSTRUMENTS). This triangular wave was amplified by a factor of 10 with an operational amplifier (137-PA05, Apex Microtechnology) and applied to the copper wire to achieve a maximum of ±50 V. The cavity resonator resonance frequency was 17.6 GHz with a Q-value of approximately 1350.
NMR signals were acquired with an OPENCORE NMR spectrometer. A solenoid coil was used as the NMR probe coil and mounted on top of the resonator. The sample was raised to the probe coil by a stepper motor within 1 second after triplet-DNP for NMR detection. A magic echo sequence was used because protons in solid samples are difficult to detect with ordinary single-pulse or spin-echo techniques due to their short T_2 relaxation time and strong dipole interactions.

Calculation of the enhancement factor.
The enhancement factor (ε) was calculated by comparing the integrated intensities of the hyperpolarized ^{1}H NMR signal of each sample after the triplet DNP sequence at 120 K and 0.66 T for pentacene and 0.65 T for DTP (Figure S8b-d) and the ^{1}H NMR signal of ethanol in thermal equilibrium at 296 K and 0.65 T (Figure S8a). To compare the enhancement factor at same temperature, the ethanol thermal was multiplied by a temperature factor of 296/120 and converted into NMR intensities at 120 K.

$$\varepsilon = \frac{N_{ref}}{N_{DNP}} \frac{T_{DNP}}{T_{ref}} \frac{g_{ref}}{g_{DNP}} \frac{E_{DNP}}{E_{ref}} \quad (1)$$

where N is the number of ^{1}H spins, T is temperature and g and E are the receiver gain and the recorded signal voltage. The ^{1}H spin polarization (P) was determined by

$$P = \varepsilon \tanh \frac{\gamma \hbar B}{2kT} \quad (2)$$

where γ, $\hbar$, B, k, T are gyromagnetic ratio, reduced Planck constant, magnetic field, Boltzmann constant and temperature, respectively.

Synthesis of 6,13-Dihydro-6,13-bis(benzothien-2-yl) pentacene-6,13-diol (2)
Benzo[b]thiophene (1.32 g, 9.8 mmol)) and dehydrated tetrahydrofuran (75 mL) were added to a 300 mL three-necked flask under argon atmosphere. After cooling to -78 °C with dry ice and acetone bath, 4 mL (10.4 mmol) of 2.6 M butyllithium hexane solution was added and stirred for 10 min. 1.0 g (3.4 mmol) of 6,13-pentacenedione (**1**) was added and stirred overnight at room temperature. The reaction was quenched with saturated ammonium chloride solution, extracted with dichloromethane, and dehydrated with sodium sulfate. After removing the solvent under reduced pressure, the resulting product was purified by silica gel chromatography (ethyl acetate: hexane = 1:4) and orange solid was obtained in a yield of 75.8%.
^{1}H NMR (400 MHz, $CDCl_3$): *δ trans*-isomer = 7.15 (s, 2H), 7.31 (m, 4H), 7.51 (s, 4H), 7.61 (q, 2H), 7.75 (d, 2H), 7.87 (q, 4H), 8.29 (s, 4H); *δ cis*-isomer = 5.95 (s, 2H), 6.58 (d, 2H), 6.67 (t, 2H), 6.87 (t, 2H), 7.31 (m, 2H), 7.65-7.75 (m, 4H), 8.06 (q, 4H), 8.66 (s, 4H).

Synthesis of 6,13-bis(benzo[b]thiophen-2-yl) pentacene (DBTP) (3)
The compound (**2**) (300 mg, 0.52 mmol), NaI (538.1 mg, 3.59 mmol), and $NaH_2PO_2 \cdot 2H_2O$ (613.7 mg, 4.95 mmol) were added to a 50 mL three-necked flask under a nitrogen atmosphere. Acetic acid (15 mL) was added and refluxed at 130 °C for 1 hour. The precipitate was isolated by filtration and washed with purified water and methanol. The crude product was purified by recrystallization with dichlorobenzene and sublimation yielding a dark blue solid in a yield of 80.7%.
^{1}H NMR (400 MHz, CD_2Cl_2): δ = 8.61 (s, 4H), 8.04 (t, J = 8.7 Hz, 4H), 7.76 (q, J = 3.2 Hz, 4H), 7.67 (s, 2H), 7.53 (quin, J = 8.7 Hz, 4H), 7.26 (q, J = 2.7 Hz, 4H). Elemental analysis: Found. C 84.04%, H 3.86%, N 0.05%; Calcd. for $C_{38}H_{22}S_2$: C 84.10%, H 4.09%, N 0.00%.

Synthesis of Synthesis of 6,13-Dihydro-6,13-dithien-2-ylpentacene-6,13-diol (4)
Thiophene (0.78 mL, 9.8 mmol) and dehydrated tetrahydrofuran (75 mL) were added to a 300 mL three-necked flask. After cooling to -78 °C with acetone and dry ice bath, 2.6 M butyllithium hexane

solution (4 mL, 10.4 mmol) solution was added and stirred for 10 min. 6,13-pentacenequinone (**1**) (1.0 g, 3.4 mmol) was added and stirred overnight at room temperature. The reaction was quenched with saturated ammonium chloride solution, extracted with dichloromethane, and dehydrated with sodium sulfate. After removing the solvent under reduced pressure, the resulting product was purified by silica gel chromatography (dichloromethane : hexane = 9 : 1) and orange solid was obtained in a yield of 58.1%.
^{1}H NMR (400 MHz, $CDCl_3$): *δ trans*-isomer = 2.92 (s, 2H), 6.78 (d, 2H), 6.97 (t, 2H), 7.34 (d, 2H), 7.51 (q, 4H), 7.87 (q, 4H), 8.20 (s, 4H); δ *cis*-isomer = 3.12 (s, 2H), 5.90 (d, 2H), 6.29 (t, 2H), 6.90 (d, 2H), 7.59 (q, 4H), 8.00 (q, 4H), 8.59 (s, 4H).

Synthesis of 6,13-di(thiophen-2-yl) pentacene (DTP) (5)
The compound (**4**) (491 mg, 1.03 mmol), NaI (1.06 g, 7.06 mmol), $NaH_2PO_2{\cdot}2H_2O$ (1.19 g, 13.5 mmol) were added to a 100 mL three-necked flask under a nitrogen atmosphere. Acetic acid (25 mL) was added and refluxed at 130 °C for 1 hour. The precipitate was isolated by filtration and washed with purified water and methanol. The crude product was purified by recrystallization with dichlorobenzene and sublimation yielding a dark blue solid in a yield of 68.2%.
^{1}H NMR (400 MHz, CD_2Cl_2): *δ* = 8.52 (s, 4H), 7.83-7.80 (m, 6H), 7.48 (dd, *J* = 3.2 Hz, 2H), 7.42 (d, 2H), 7.31 (q, *J* = 3.2 Hz, 4H). Elemental analysis: Found. C 81.42%, H 3.86%, N 0.08%; Calcd. for $C_{30}H_{18}S_2$: C 81.41%, H 4.10%, N 0.00%.

Synthesis of Synthesis of 6,13-di(benzofuran-2-yl)-5a,6,13,13a-tetrahydropentacene-6,13-diol (6)
Benzofuran (1.15 g, 10 mmol) was added to a 300 mL three-necked flask under a nitrogen atmosphere. After cooling to -78 °C, 2.6 M butyllithium hexane solution 3.85 mL (10 mmol) was added and stirred for 1 hour. 6,13-pentacenequinone (**1**) (1.0 g, 3.2 mmol), dehydrated tetrahydrofuran (75 mL) was added and stirred overnight at room temperature. The reaction was quenched by adding 30 mL saturated ammonium chloride solution, extracted with 20 mL toluene and dehydrated with sodium sulfate. After removal of the solvent under reduced pressure, a black solid was obtained.

Synthetic scheme of 6,13-di(benzofuran-2-yl) pentacene (7)
The compound (**6**) (2.26 g, 4.15 mmol), dehydrated tetrahydrofuran (80 mL) was added to a 300 mL three-neck flask and bubbled with Ar. $Sn_2Cl_2{\cdot}2H_2O$ (6.1 g, 7.5 mmol), 35% HCl (60 mL) was added and stirred overnight. After filtration of the precipitate and washing with methanol, a purple solid was obtained in a yield of 41.1%.
^{1}H NMR (400 MHz, CD_2Cl_2): *δ* = 8.67 (s, 4H), 7.86 (d, *J* = 6.0 Hz, 2H), 7.81 (q, *J* = 3.2 Hz, 4H), 7.72 (d, *J* =8.2 Hz, 2H), 7.46 (quin, *J* = 7.32 Hz, 4H), 7.34 (s, 2H), 7.30 (dd, *J* = 2.7 Hz, 4H). EA: Found. C 89.37%, H 4.28%, N 0.00%; Calcd. for $C_{38}H_{22}O_2$: C 89.39%, H 4.34%, N 0.00%.

Computational details
Geometry optimization, ISC rate constant and SOCME calculations were carried out using time-dependent density functional theory (TDDFT) of the ORCA 5.0.3 program package[4,5]. We used LC-BLYP functional[6] with the range separation parameter $\mu = 0.15$ and def2-TZVP basis sets[7–9].
DMRG-CASSCF[10–12] calculations were carried out using PySCF[13–15] and BLOCK2[16] program package, and then ZFS *D*-tensors were calculated according to the reported formula[17]. We used cc-pVDZ basis sets in the series of calculations.

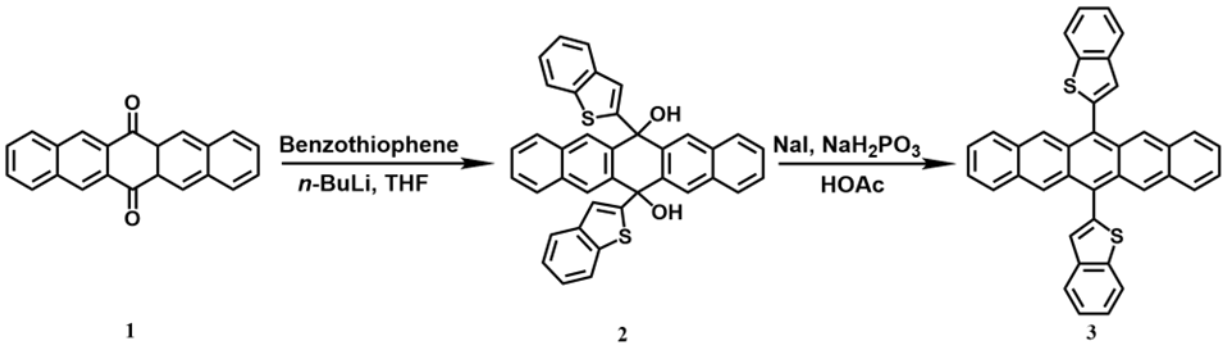

Scheme S1. Synthetic scheme of 6,13-bis(benzo[b]thiophen-2-yl) pentacene (DBTP)

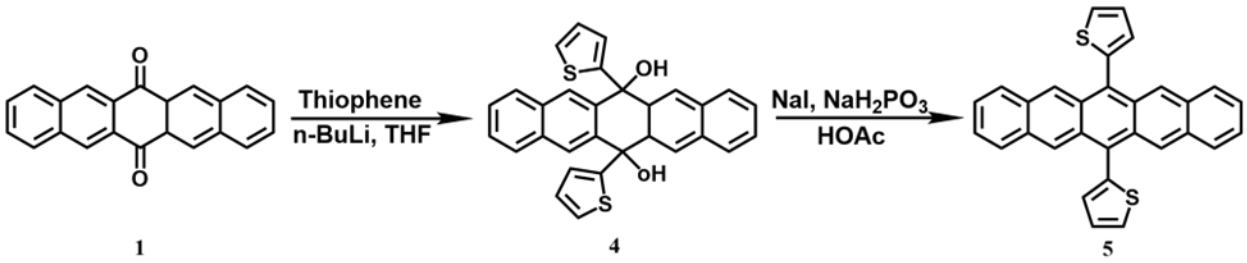

Scheme S2. Synthetic scheme of 6,13-di(thiophen-2-yl) pentacene (DTP)

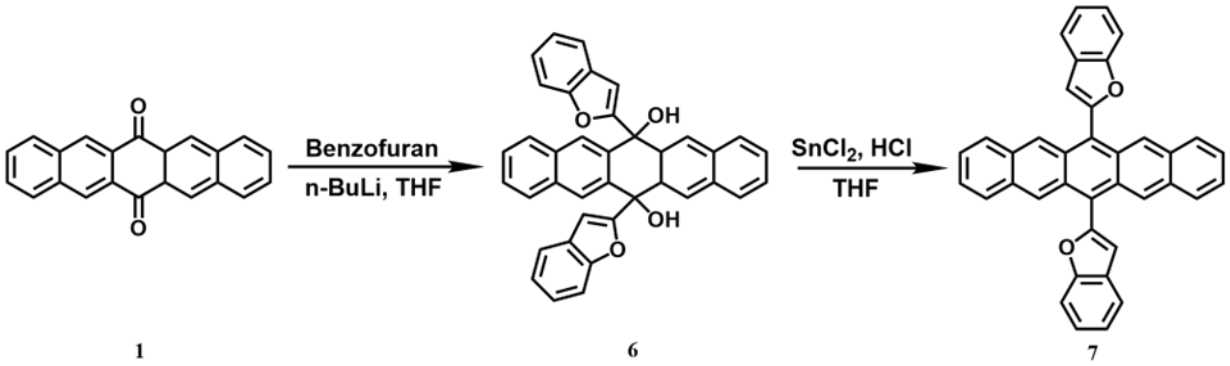

Scheme S3. Synthetic scheme of 6,13-di(benzofuran-2-yl) pentacene (DBFP)

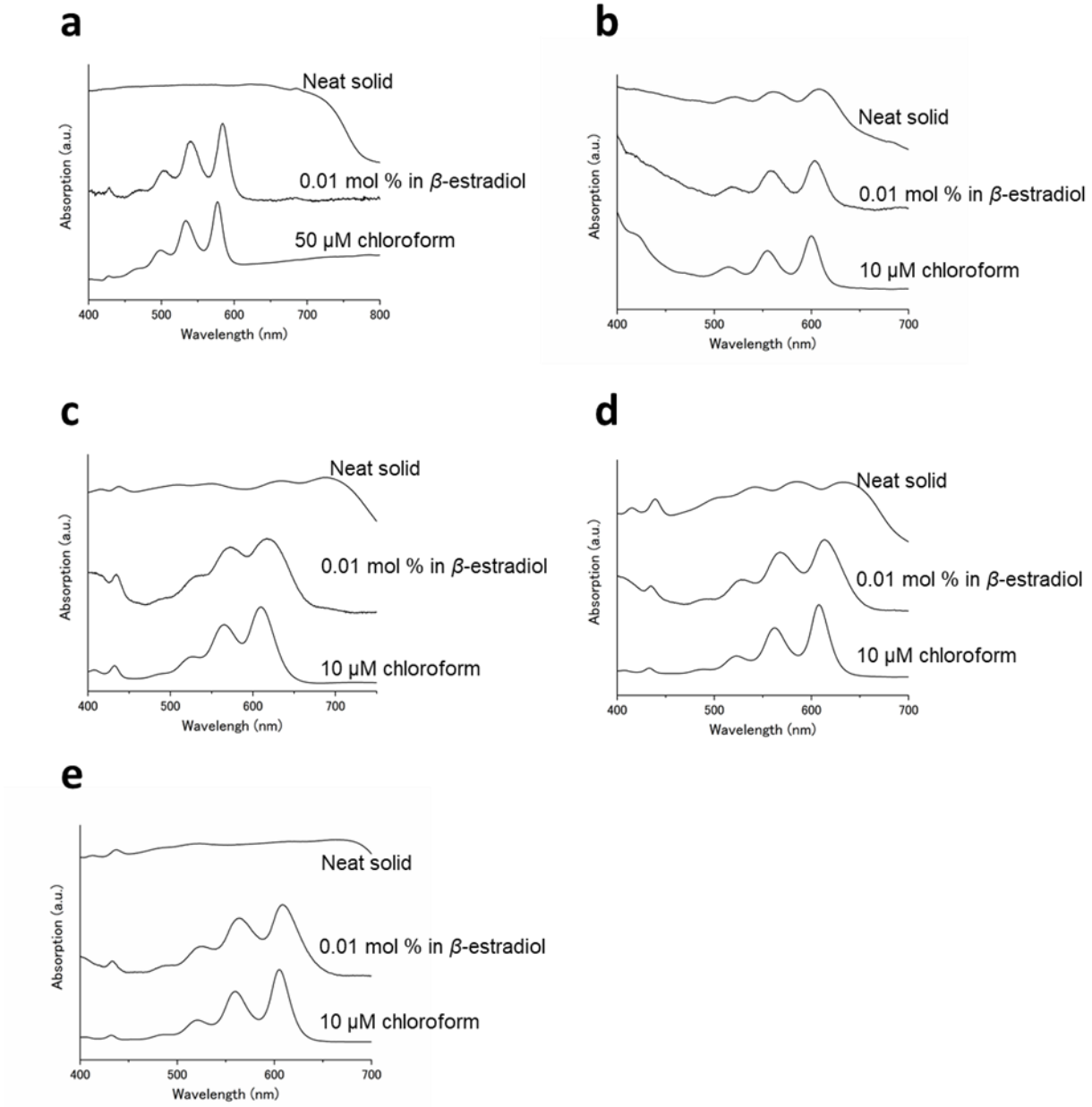

Fig. S1. Absorption spectra of a) pentacene, b) DPP, c) DBFP, d) DBTP and e) DTP in chloroform solution, *β*-estradiol glass, and neat solids at room temperature.

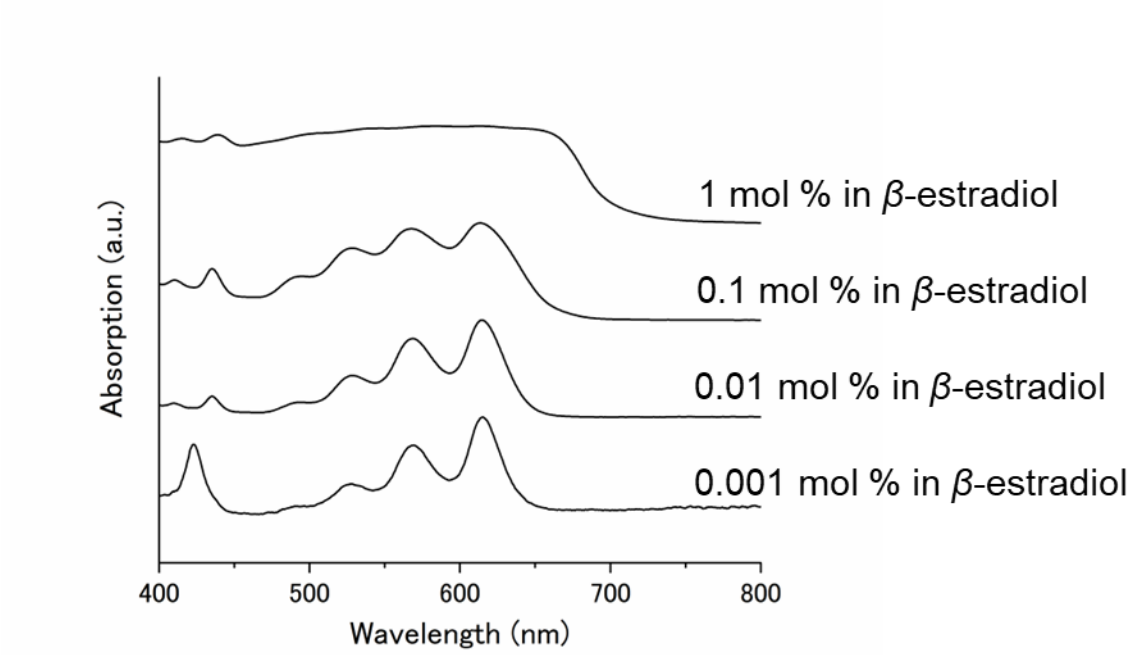

Fig. S2. Concentration-dependent absorption spectra of DBTP in *β*-estradiol glass at room temperature.

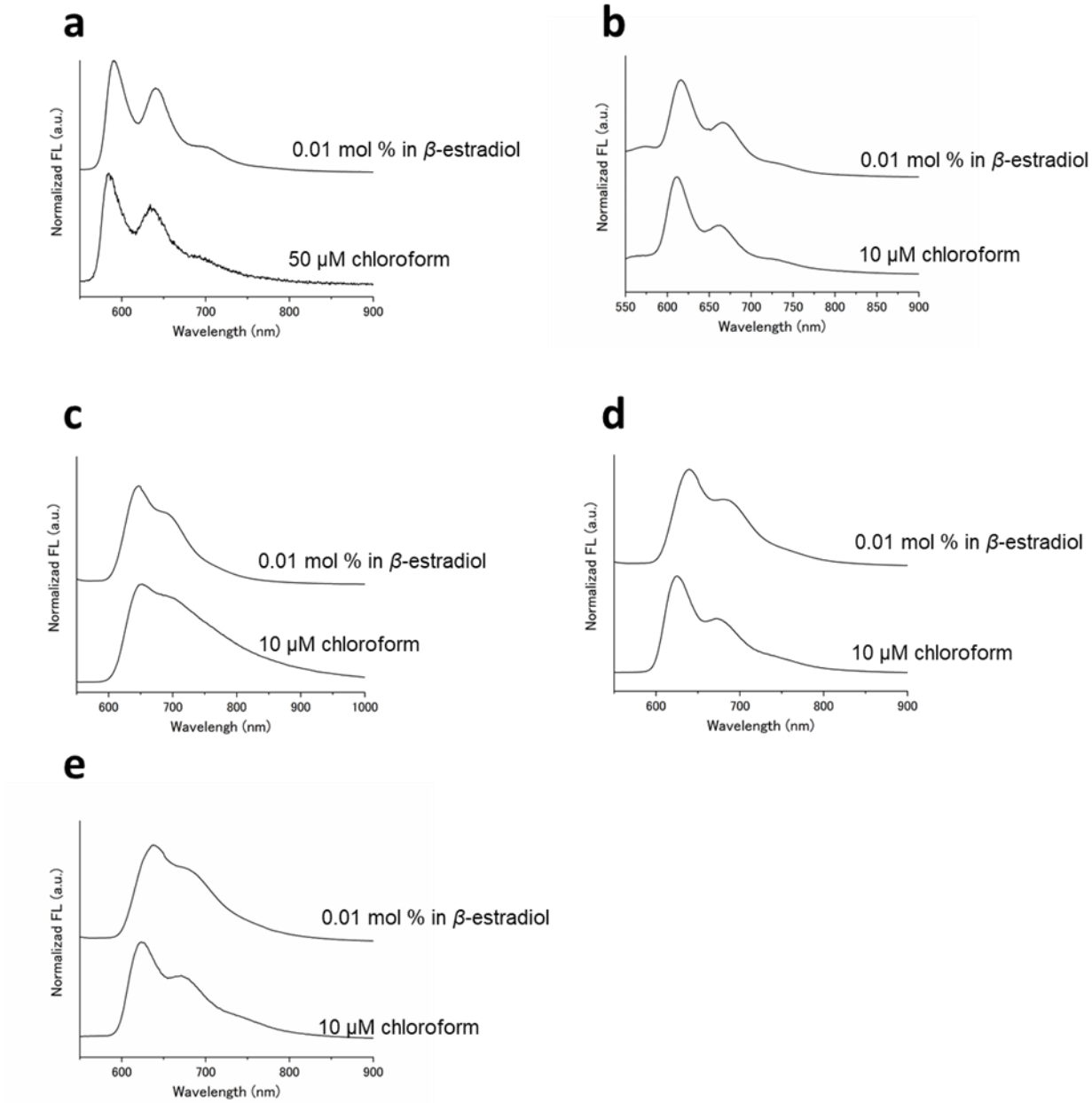

Fig. S3. Fluorescence spectra of a) pentacene (λ_{ex} = 500 nm), b) DPP (λ_{ex} = 520 nm), c) DBFP (λ_{ex} = 525 nm), d) DBTP (λ_{ex} = 523 nm) and e) DTP (λ_{ex} = 520 nm) in chloroform solution and *β*-estradiol glass at room temperature.

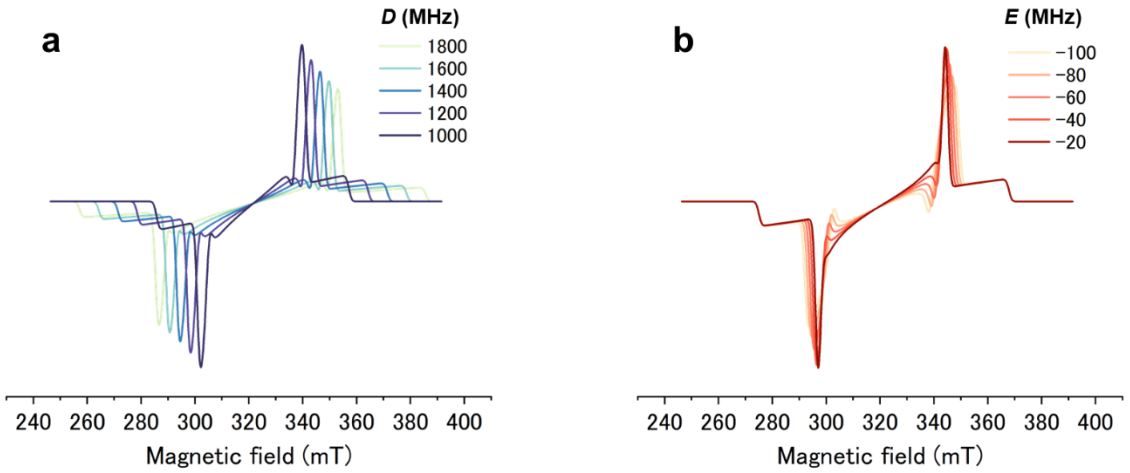

Fig. S4. ESR simulation with changing a) only the *D* and b) *E* value, respectively, while the other parameters are fixed (g = 2, B = 9.0 GHz, p_x = 0.4, p_y = 0.2, p_z = 0.2).

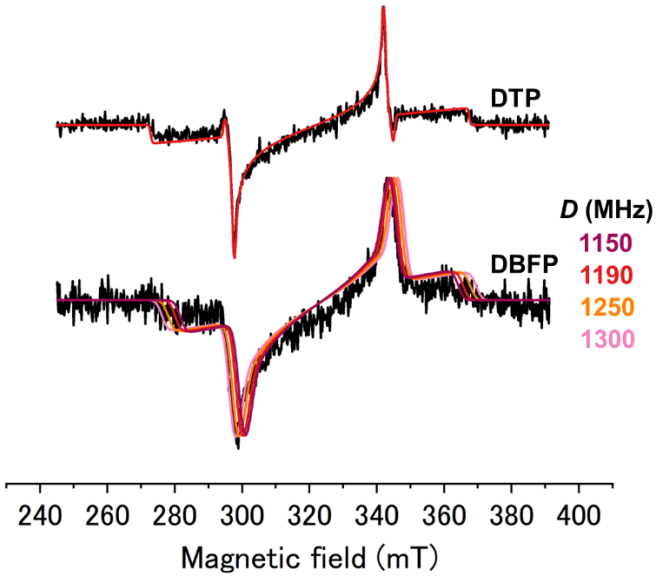

Fig. S5. Normalized time-resolve ESR spectra of DBFP and DTP doped in *β*-estradiol at room temperature. Red lines show simulation with EasySpin toolbox in Mathlab. Simulations were performed with different *D* values for DBFP (Other parameters were set to $|E| = 45.1$, $p_x = 0.60$, $p_y = 0.26$, $p_z = 0.14$).

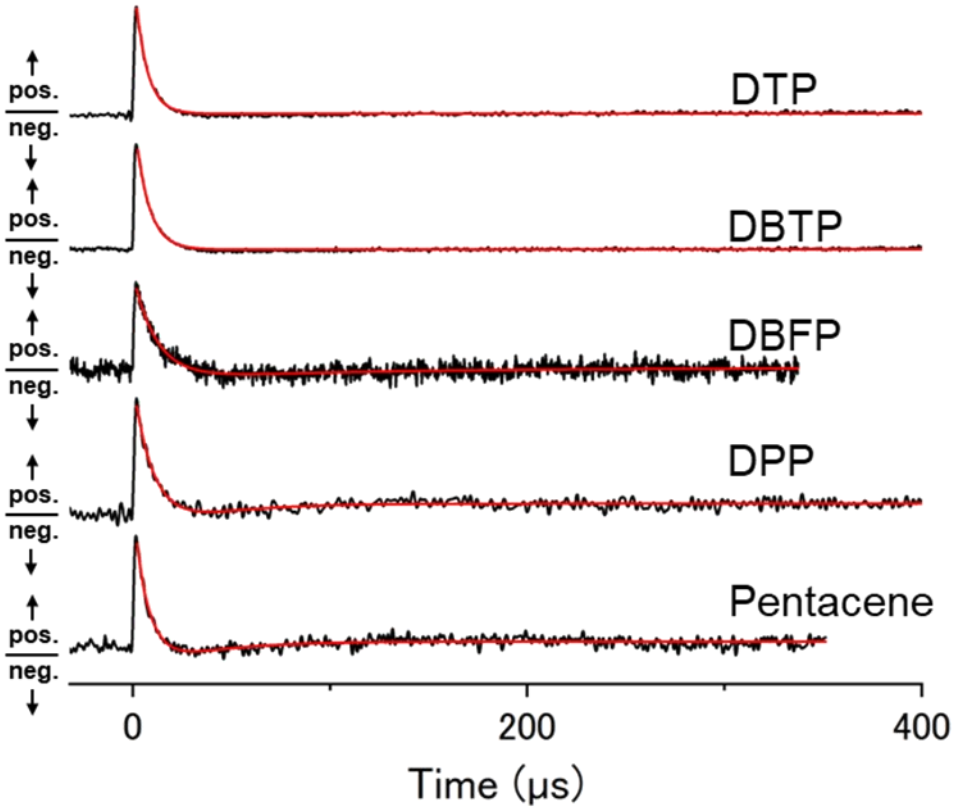

Fig. S6. ESR signal decays at the peak top of the ESR spectrum under pulsed irradiation at 527 nm for each polarizing agent in *β*-estradiol glass at a concentration of 0.01 mol% at room temperature. Red lines show single exponential fitting results. The fitting result for the red line is the following equation, $A \exp(-t/\tau_A) + B \exp(-t/\tau_B) + C$. Fitting parameters are shown in Table S2.

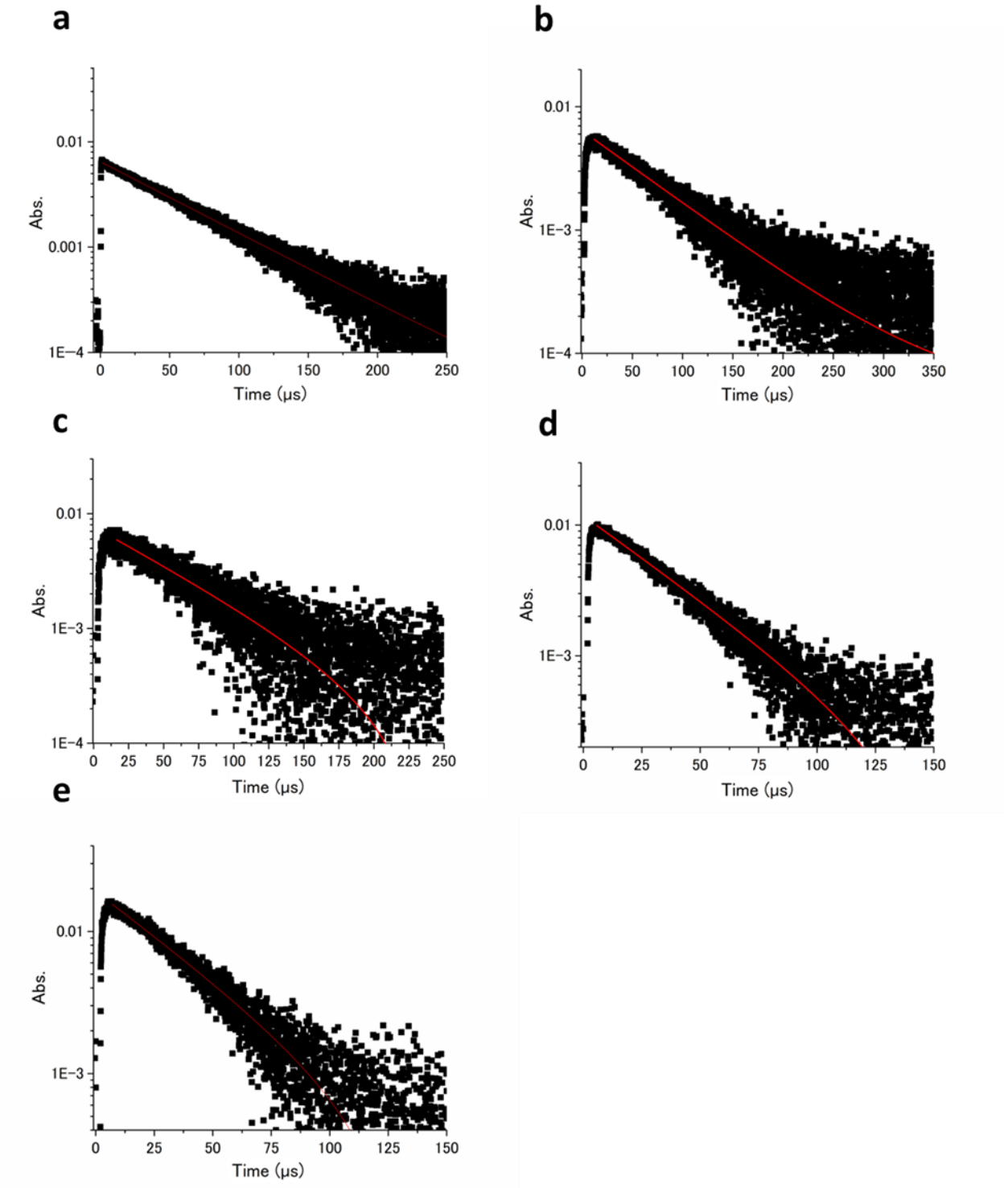

Fig. S7. Transient absorption decays of a) pentacene, b) DPP, c) DBFP, d) DBTP and e) DTP in *β*-estradiol glass at a concentration of 0.01 mol% at room temperature (excited at 527 nm, monitored at 510 nm).

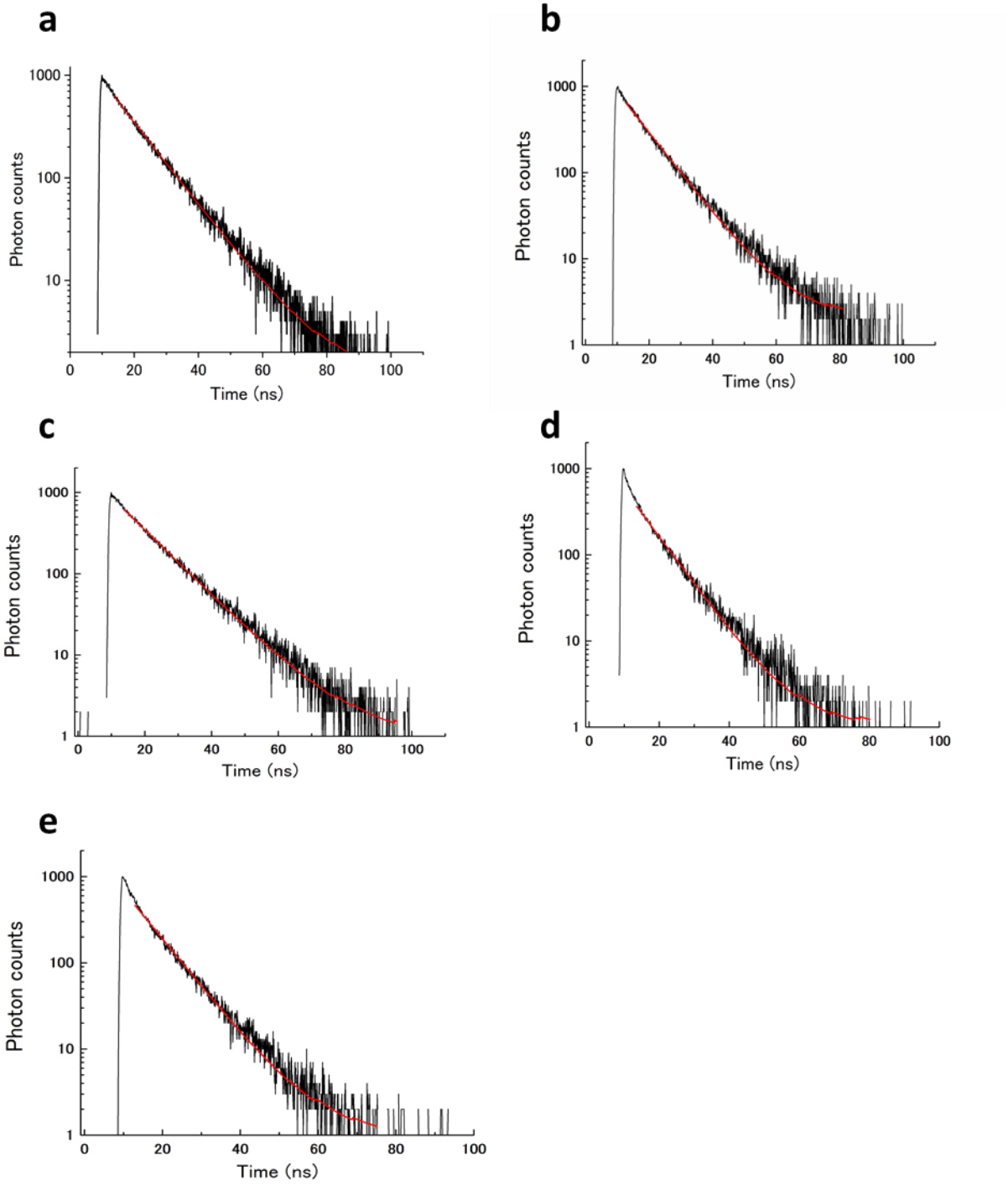

Fig. S8. Fluorescence lifetime of a) pentacene, b) DPP and c) DBFP, d) DBTP and e) DTP in *β*-estradiol glass at a concentration of 0.01 mol% at room temperature.

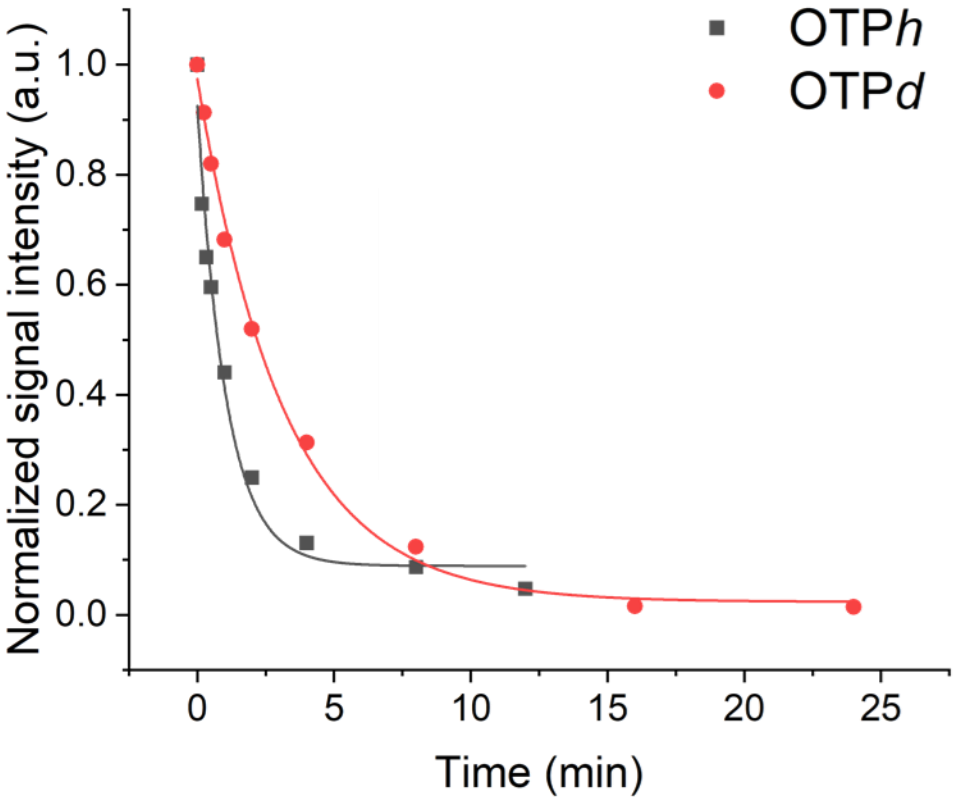

Fig. S9. ^{1}H NMR signal decays of OTP (black) and partially deuterated OTP (OTP : [D14]OTP : = 10 : 90 wt%) doped with 0.07 mol % DTP at different time intervals from triplet-DNP to NMR measurements.

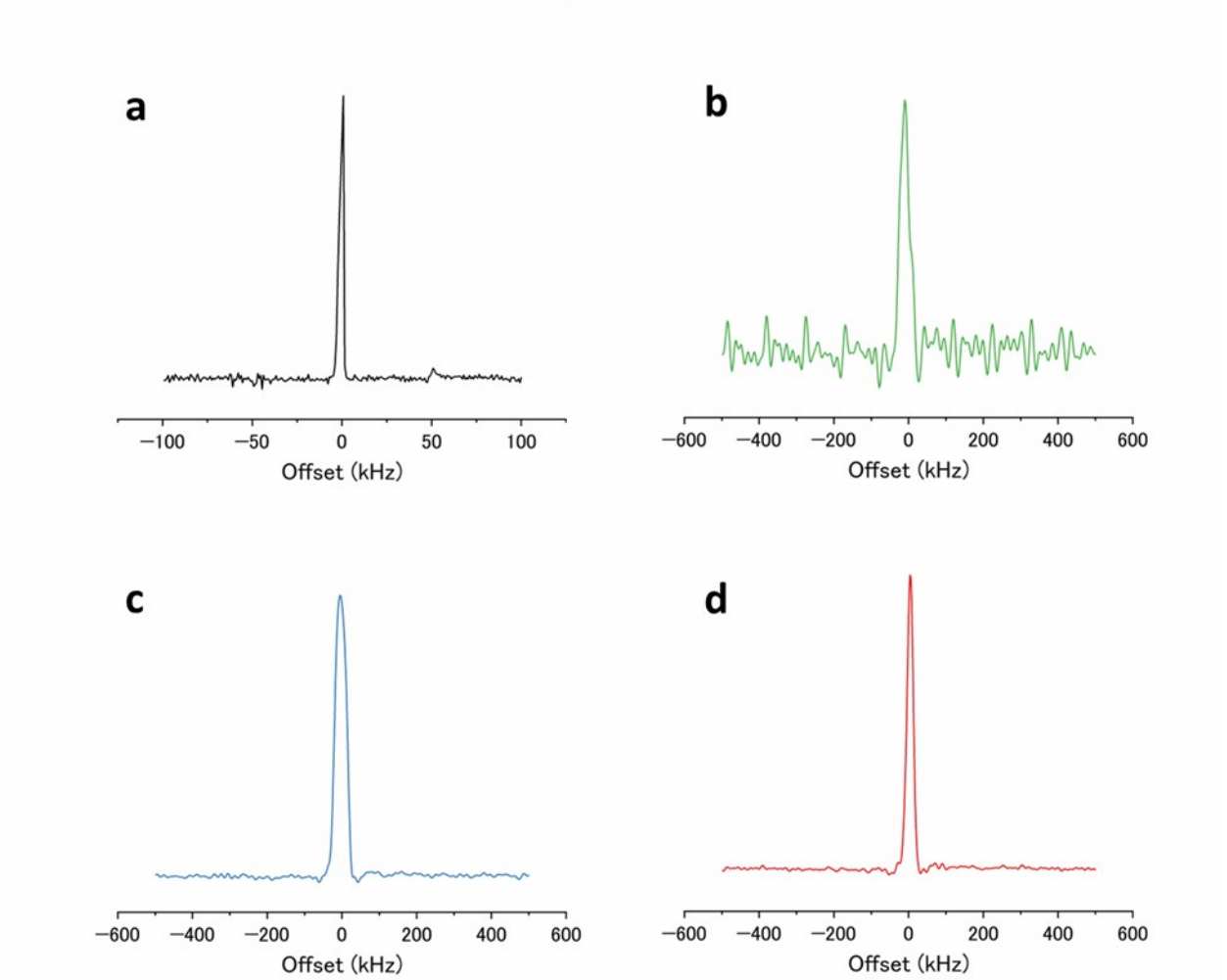

Fig. S10. a) ^{1}H NMR spectrum of ethanol in the thermal equilibrium at 296 K with 10 times multiplication used as a reference. ^{1}H NMR spectra of b) OTP doped with 0.05 mol% pentacene, c) OTP doped with 0.07 mol% DTP, and d) partially deuterated OTP (OTP : [D14]OTP = 10 : 90 wt%) doped with 0.07 mol% DTP after the triplet-DNP process for 5 min at 120 K.

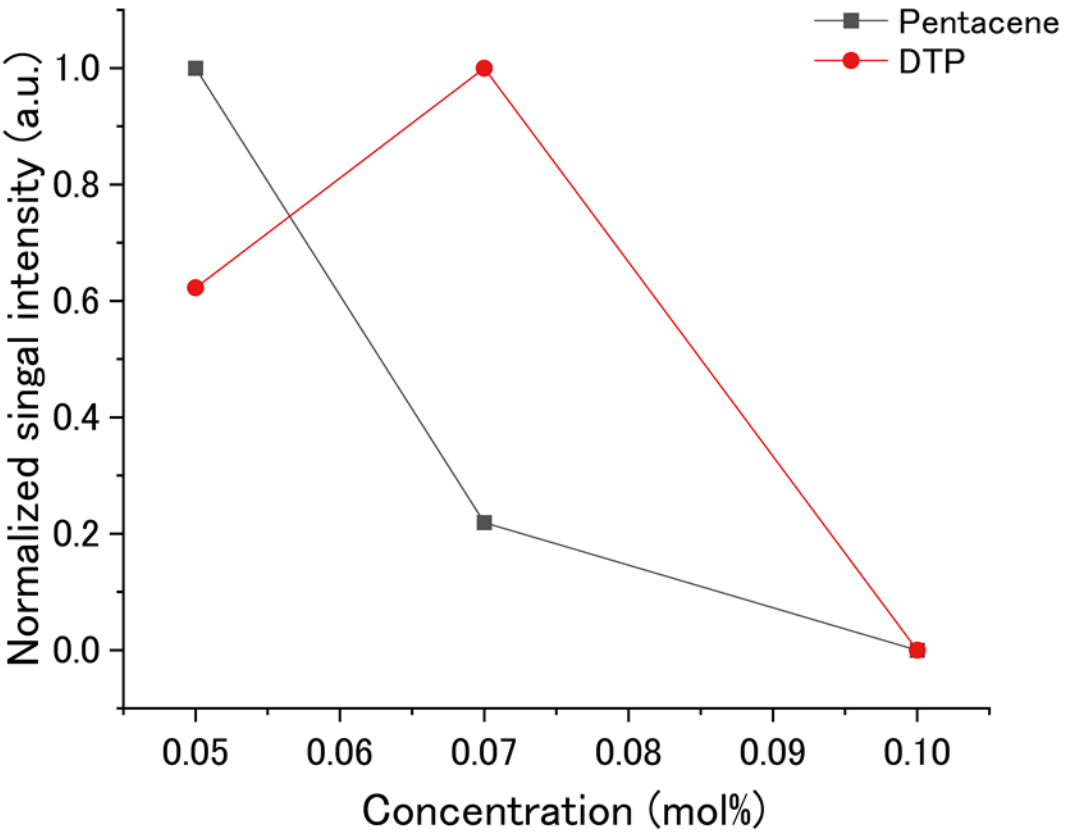

Fig. S11. Concentration dependence of ^{1}H-NMR signal intensity of OTP doped with pentacene (black) and DTP (red) after the triplet-DNP.

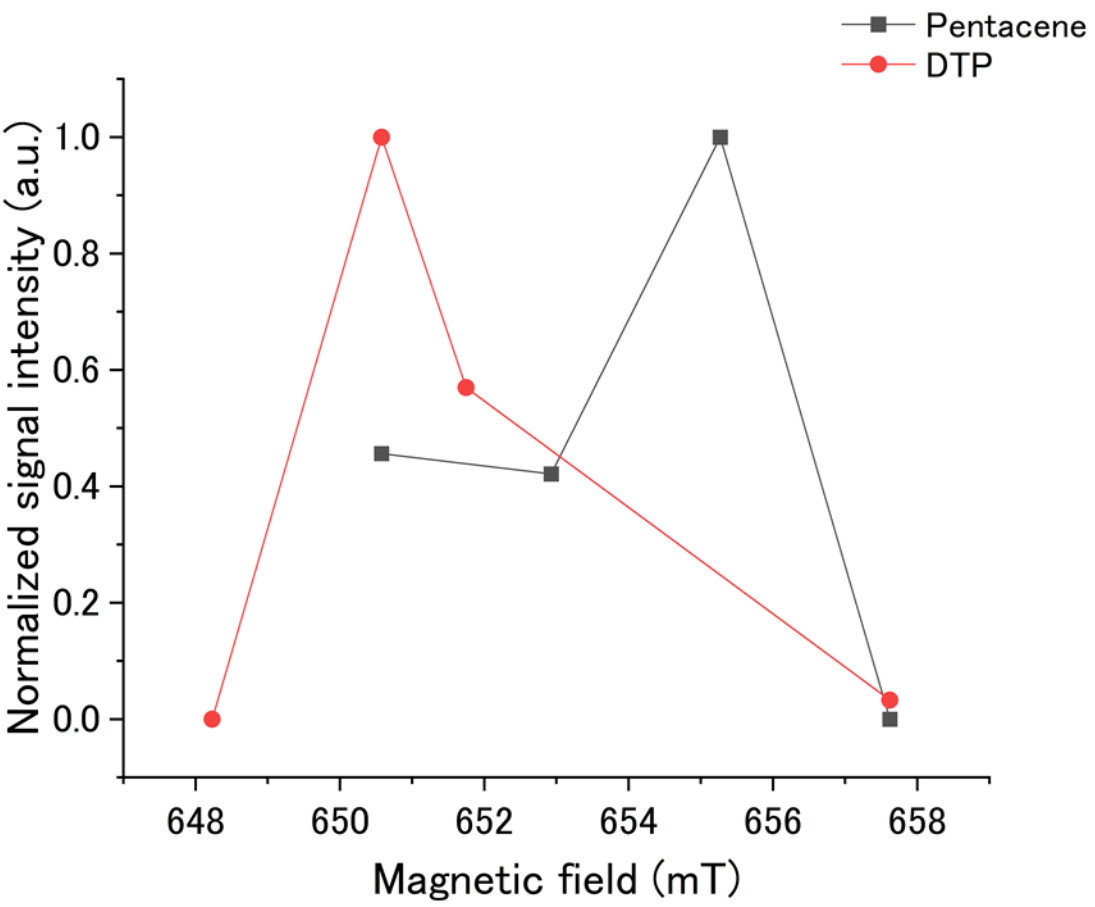

Fig. S12. Magnetic field dependence of ^{1}H-NMR signal intensity of OTP doped with 0.05 mol% pentacene (black) and DTP (red) after the triplet-DNP.

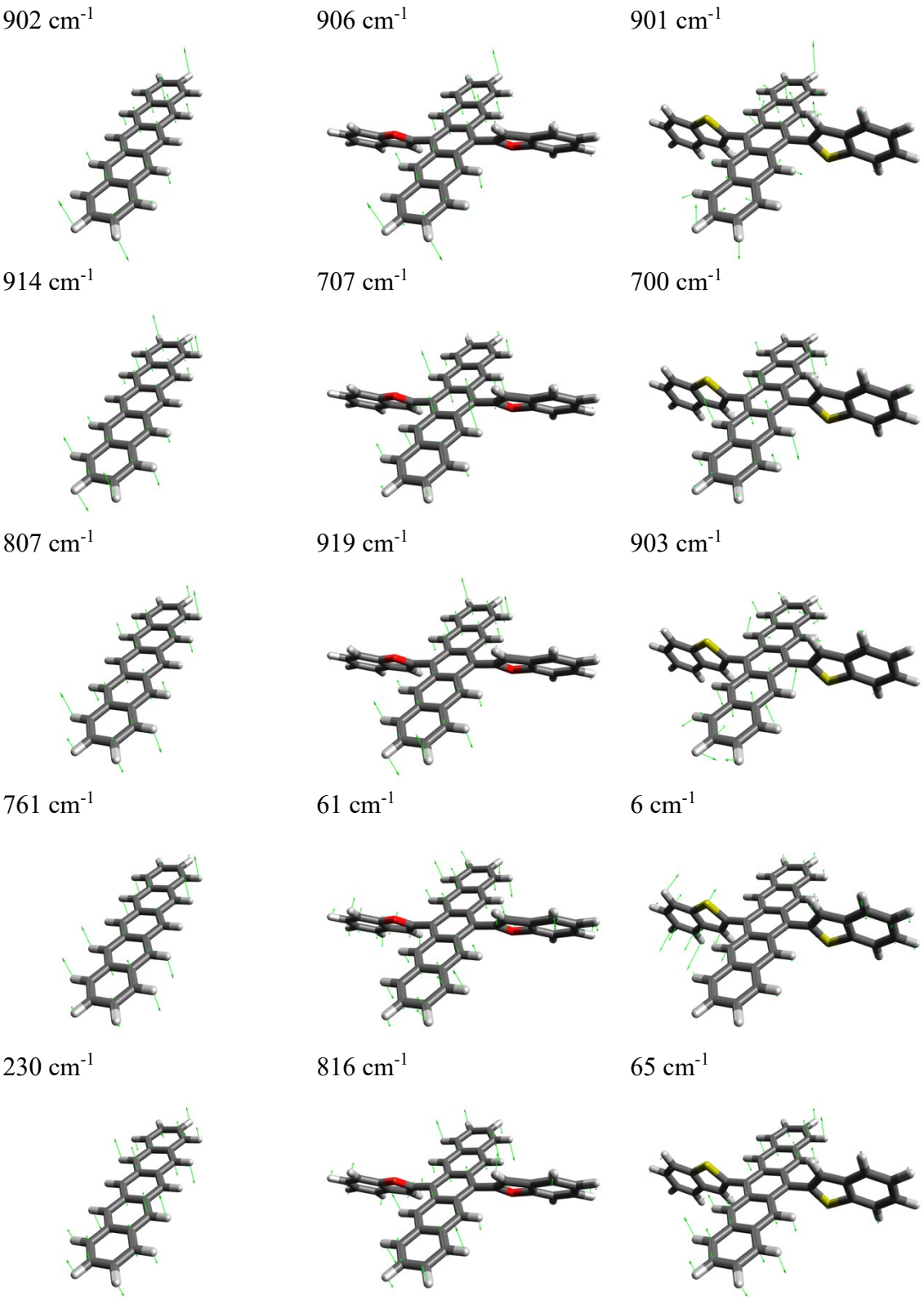

Fig. S13. Top 5 normal modes that enhance X-direction of SOCME.

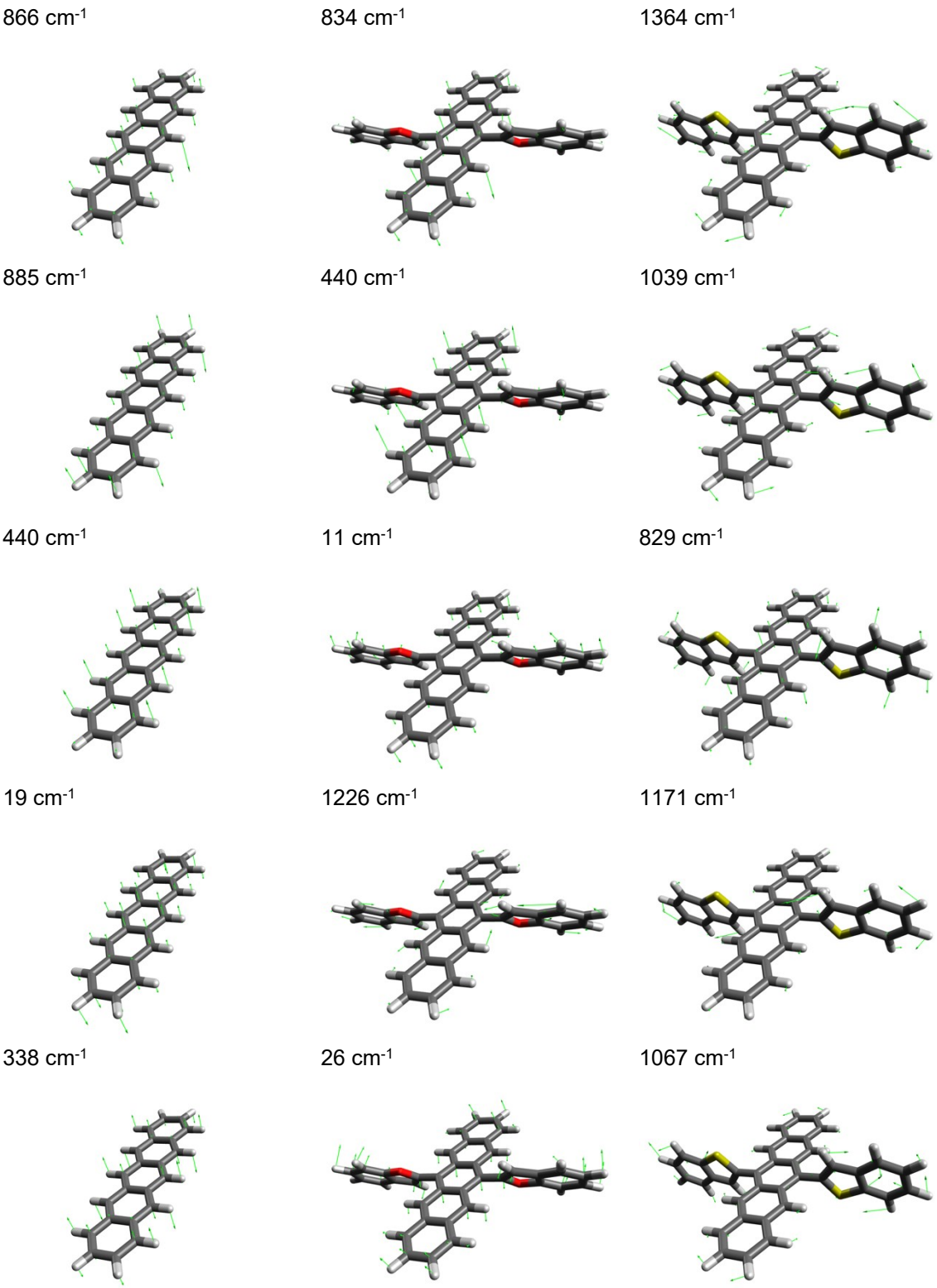

Fig. S14. Top 5 normal modes that enhance Y-direction of SOCME.

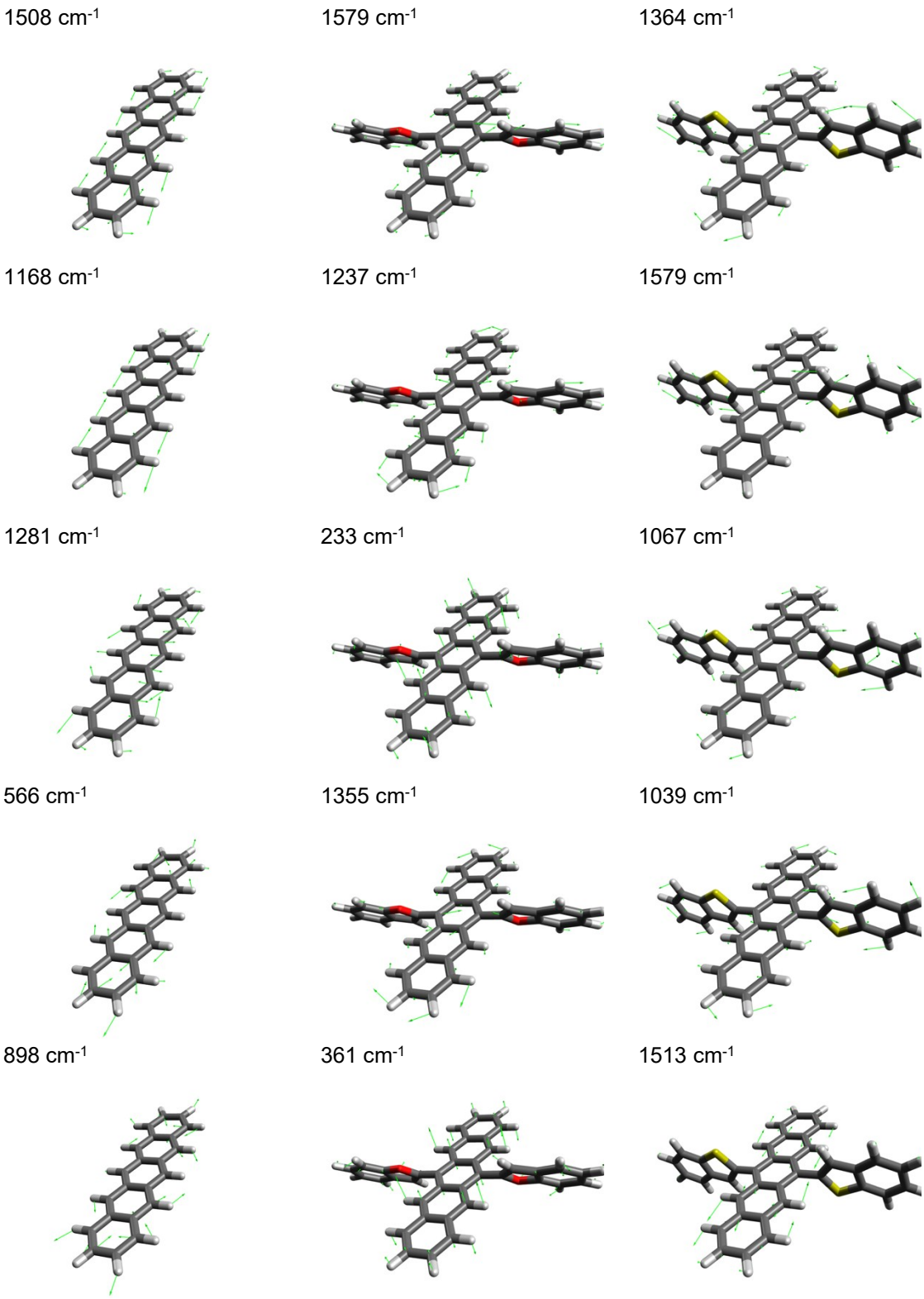

Fig. S15. Top 5 normal modes that enhance Z-direction of SOCME.

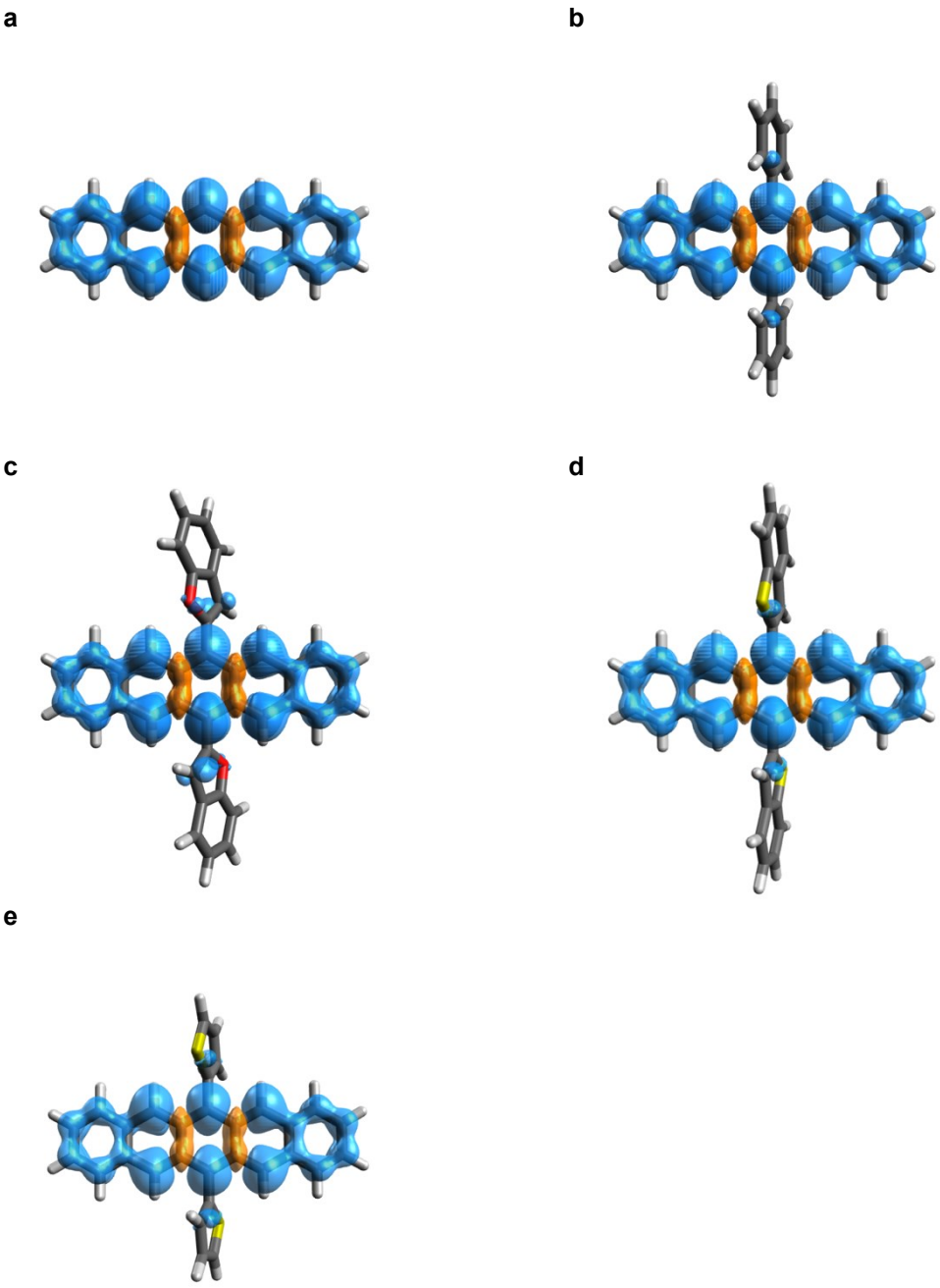

Fig. S16. Spin density distributions of a) pentacene, b) DPP, c) DBFP, d) DBTP and e) DTP calculated at DMRG-CASSCF(22e, 22o)/cc-pVDZ level. The isovalue is 0.0008.

Table S1. Fluorescence quantum yield Φ_{FL}, triplet quantum yield Φ_T, fluorescence lifetime τ_{FL} triplet lifetime τ_T and spin-lattice relaxation times T_{1e} of pentacene, DPP, DBFP, DBTP, DTP in β-estradiol glass at a concentration of 0.01 mol%.

	Pentacene	DPP	DBFP	DBTP	DTP
Φ_{FL}	10	16	38	18	16
Φ_T *	90	84	62	82	84
τ_{FL} (ns)	8.4	9.2	10.8	7.9	7.9
τ_T (µs)	64	73	65	34	35
T_{1e} (µs)	7.7	10.2	10.2	7.5	6.7

*Triplet quantum yields were calculated assuming other deactivation pathways negligible.

Table S2. Fitting parameters for signal decay of ESR spectra in *β*-estradiol glass at a concentration of 0.01 mol% for each of the polarization sources in Figure S5.

	A	τ_A (µs)	B	τ_B (µs)
Pentacene	0.020	10.2	-0.0047	34
DPP	0.057	7.7	-0.011	32
DBFP	0.028	11.8	-0.0032	101
DBTP	0.13	7.5	-0.0037	101
DTP	0.096	6.7	-0.0032	86

Table S3. Derivatives of the SOCMEs along 5 normal modes with the strongest enhancement of the SOCMEs in the X-direction of pentacene, DBFP and DBTP.

ω_k / cm^{-1}	$\partial_{q_k} V_0^X$ / $i\ cm^{-1}$	$\partial_{q_k} V_0^Y$ / $i\ cm^{-1}$	$\partial_{q_k} V_0^Z$ / $i\ cm^{-1}$
Pentacene			
902	0.358	0.002	0.000
914	0.354	0.003	0.000
807	0.141	0.004	0.000
761	0.126	0.003	0.000
230	0.122	0.003	0.000
DBFP			
906	0.249	0.004	0.005
707	0.226	0.051	0.001
919	0.202	0.001	0.007
61	0.135	0.027	0.020
816	0.112	0.049	0.016
DBTP			
901	0.175	0.073	0.025
700	0.173	0.048	0.046
903	0.167	0.067	0.049
6	0.122	0.056	0.034
65	0.121	0.046	0.041

Table S4. Derivatives of the SOCMEs along 5 normal modes with the strongest enhancement of the SOCMEs in the Y-direction of pentacene, DBFP and DBTP.

$\omega_k \,/\, cm^{-1}$	$\partial_{q_k} V_0^X \,/\, i\ cm^{-1}$	$\partial_{q_k} V_0^Y \,/\, i\ cm^{-1}$	$\partial_{q_k} V_0^Z \,/\, i\ cm^{-1}$
Pentacene			
866	0.000	0.249	0.000
885	0.000	0.136	0.000
440	0.000	0.084	0.000
19	0.000	0.077	0.000
338	0.001	0.031	0.000
DBFP			
834	0.009	0.127	0.002
440	0.004	0.103	0.019
11	0.002	0.057	0.002
1226	0.010	0.055	0.005
26	0.005	0.053	0.004
DBTP			
1364	0.003	0.281	0.169
1039	0.007	0.253	0.130
829	0.012	0.201	0.021
1171	0.001	0.201	0.105
1067	0.003	0.194	0.155

Table S5. Derivatives of the SOCMEs along 5 normal modes with the strongest enhancement of the SOCMEs in the Z-direction of pentacene, DBFP and DBTP.

ω_k / cm^{-1}	$\partial_{q_k} V_0^X$ / $i\ cm^{-1}$	$\partial_{q_k} V_0^Y$ / $i\ cm^{-1}$	$\partial_{q_k} V_0^Z$ / $i\ cm^{-1}$
Pentacene			
1508	0.000	0.002	0.007
1168	0.000	0.003	0.002
1281	0.000	0.002	0.002
566	0.000	0.002	0.002
898	0.002	0.000	0.002
DBFP			
1579	0.042	0.003	0.029
1237	0.004	0.045	0.029
233	0.031	0.026	0.026
1355	0.017	0.004	0.024
361	0.000	0.025	0.022
DBTP			
1364	0.003	0.281	0.169
1579	0.010	0.144	0.156
1067	0.003	0.194	0.155
1039	0.007	0.253	0.130
1513	0.003	0.183	0.128

SI References

Sample References:

1. Vets, N.; Smet, M.; Dehaen, W. Reduction versus Rearrangement of 6,13-Dihydro-6,13-Diarylpentacene-6,13-Diols Affording 6,13- and 13,13'-Substituted Pentacene Derivatives. *Synlett*. **2005**, 217–222.
2. Fujiwara, S.; Matsumoto, N.; Nishimura, K.; Kimizuka, N.; Tateishi, K.; Uesaka, T.; Yanai, N. Triplet Dynamic Nuclear Polarization of Guest Molecules through Induced Fit in a Flexible Metal–Organic Framework. *Angew. Chem. Int. Ed.* **2022**, *61* (9).
3. Takeda, K. OPENCORE NMR: Open-source core modules for implementing an integrated FPGA-based NMR spectrometer. *J. Magn. Reson.* **2008**, *192* (2), 218–229.
4. Neese, F. The ORCA program system. *WIREs Comput. Mol. Sci.* **2012**, *2* (1), 73–78.
5. Neese, F.; Wennmohs, F.; Becker, U.; Riplinger, C. The ORCA quantum chemistry program package. *J. Chem. Phys.* **2020**, *152* (22), 224108.
6. Tawada, Y.; Tsuneda, T.; Yanagisawa, S.; Yanai, T.; Hirao, K. A long-range-corrected time-dependent density functional theory. *J. Chem. Phys.* **2004**, *120* (18), 8425–8433.
7. Weigend, F.; Ahlrichs, R. Balanced basis sets of split valence, triple zeta valence and quadruple zeta valence quality for H to Rn: Design and assessment of accuracy. *Phys. Chem. Chem. Phys.* **2005**, *7* (18), 3297.
8. Weigend, F. Accurate Coulomb-fitting basis sets for H to Rn. *Phys. Chem. Chem. Phys.* **2006**, *8* (9), 1057.
9. Hellweg, A.; Hättig, C.; Höfener, S.; Klopper, W. Optimized sccurate auxiliary basis sets for RI-MP2 and RI-CC2 calculations for the atoms Rb to Rn. *Theor. Chem. Acc.* **2007**, *117* (4), 587–597.
10. Ghosh, D.; Hachmann, J.; Yanai, T.; Chan, G. K.-L. Orbital optimization in the density matrix renormalization group, with applications to polyenes and β -Carotene. *J. Chem. Phys.* **2008**, *128* (14), 144117.
11. Zgid, D.; Nooijen, M. The density matrix renormalization group self-consistent field method: Orbital optimization with the density matrix renormalization group method in the active space. *J. Chem. Phys.* **2008**, *128* (14), 144116.
12. Yanai, T.; Kurashige, Y.; Ghosh, D.; Chan, G. K.-L. Accelerating convergence in iterative solution for large-scale complete active space self-consistent-field calculations. *Int. J. Quantum Chem.* **2009**, *109* (10), 2178–2190.
13. Sun, Q.; Berkelbach, T. C.; Blunt, N. S.; Booth, G. H.; Guo, S.; Li, Z.; Liu, J.; McClain, J. D.; Sayfutyarova, E. R.; Sharma, S.; Wouters, S.; Chan, G. K. P Y SCF: The Python-based Simulations of Chemistry Framework. *WIREs Comput. Mol. Sci.* **2018**, *8* (1).
14. Sun, Q.; Zhang, X.; Banerjee, S.; Bao, P.; Barbry, M.; Blunt, N. S.; Bogdanov, N. A.; Booth, G. H.; Chen, J.; Cui, Z.-H.; Eriksen, J. J.; Gao, Y.; Guo, S.; Hermann, J.; Hermes, M. R.; Koh, K.; Koval, P.; Lehtola, S.; Li, Z.; Liu, J.; Mardirossian, N.; McClain, J. D.; Motta, M.; Mussard, B.; Pham, H. Q.; Pulkin, A.; Purwanto, W.; Robinson, P. J.; Ronca, E.; Sayfutyarova, E. R.; Scheurer, M.; Schurkus, H.

F.; Smith, J. E. T.; Sun, C.; Sun, S.-N.; Upadhyay, S.; Wagner, L. K.; Wang, X.; White, A.; Whitfield, J. D.; Williamson, M. J.; Wouters, S.; Yang, J.; Yu, J. M.; Zhu, T.; Berkelbach, T. C.; Sharma, S.; Sokolov, A. Yu.; Chan, G. K.-L. Recent developments in the PySCF program package. *J. Chem. Phys.* **2020**, *153* (2), 024109.
15. Sun, Q. Libcint: An efficient general integral library for Gaussian basis functions. *J. Comput. Chem.* **2015**, *36* (22), 1664–1671.
16. Zhai, H.; Chan, G. K.-L. Low communication high performance *an initio* density matrix renormalization group algorithms. *J. Chem. Phys.* **2021**, *154* (22), 224116.
17. Ganyushin, D.; Gilka, N.; Taylor, P. R.; Marian, C. M.; Neese, F. The resolution of the identity approximation for calculations of spin-spin contribution to zero-field splitting parameters. *J. Chem. Phys.* **2010**, *132* (14), 144111.